

Simulation of spherical rigid bodies subject to friction with multiple impacts

Eliana Sanchez¹, Alberto Cardona¹, Alejandro Cosimo², Olivier Brùls², Federico Cavaliere¹

¹ Centro de Investigación de Métodos Computacionales (CIMEC)
Universidad Nacional del Litoral-CONICET
Santa Fe, Argentina
[esanchez,acardona,fcavaliere]@cimec.unl.edu.ar

²Department of Aerospace and Mechanical Engineering
University of Liège
Liège, Belgium
[acosimo,o.bruls]@uliege.be

ABSTRACT

This work presents an extension of the nonsmooth generalized α time integration scheme applied to multi-impact collisions including Coulomb's friction. The classical Newton impact law is used to extend the applicability of multiple impact problems with friction in spherical bodies assuming instantaneous local impact events. The geometrical properties of the spheres are described by a rigid body formulation with translational and rotational degrees of freedom. Finally, the robustness and the performance of the proposed methodology is demonstrated by three numerical examples.

Keywords: Multi-impact collisions, Friction, Nonlinear dynamics, Impact, Implicit.

1 INTRODUCTION

The characterization of mechanical systems with multiple impacts between spherical rigid bodies under frictional contact is a challenging research topic that allows the simulation of different kinds of problems such as the typical billiard break, the Newton's cradle toy and the Bernoulli's problems, among others [1]. When a multibody system is subjected to impacts, two scenarios can arise: (i) **single impacts**, when the bodies are in contact at a single point and the impact occurs at this point, and (ii) **multiple impacts**, when there are several points in contact and the impact occurs simultaneously in some of them [2].

From a general view, there are two main approaches for numerically solving impact problems. The first approach assumes that the impact time duration is very small. This group can be even subdivided into first-order and second-order models. The first-order models can be based on Darboux [3] formulation where the normal impulse is adopted as integration variable instead of time. Another alternative is by using the Poisson local impact law, which assumes a decomposition of the impact process into a compression and an expansion phases and also involves a coefficient of restitution [2]. Recently, Liu and Brogliato have extended the first-order formulation to study granular chain problems [4]. On the other hand, the second-order models use some kind of spring-dashpot models. The second approach describes the impact process as instantaneous by using the classical Newton local impact law, which relates the pre-impact and the post-impact velocities by a restitution coefficient. The adoption of the local Newton or Poisson laws for modelling multiple impacts is a natural and convenient choice. However, additional complications appear in the formulations when frictional effects are considered because a nonlinear friction law such as the Coulomb's law is needed.

In this work, we introduce a new methodology for the simulation of multiple impact collisions with friction between spherical rigid bodies in the framework of the nonsmooth contact dynamics and the nonlinear finite element method. The proposal is an extension of the frictionless multiple

impact algorithm based on the Newton's impact law presented by Cosimo *et al.* [5] to the frictional case. The time integrator scheme used to integrate the equations of motion is the new version of the non-smooth generalised α integrator [6]. It is characterised by the solution of three decoupled sub-problems to be solved at each time step, the so-called: *smooth* motion, *position* correction and *velocity* correction sub-problems. The algorithm presented in this work to simulate multiple impact problems with friction, is based on modifying the velocity correction active set in order to define a sequence of impact problems on a vanishing time interval. Then, the active set of each velocity-level sub-problem is redefined in the normal and in the tangential directions, in such a way that closed contacts with zero pre-impact velocity are considered inactive.

The frictional contact element formulated by Cavalieri *et al.* [7] was extended to manage sliding, rolling and drilling friction effects. We use it in the numerical examples section to simulate the contact between a sphere and a rigid plane. Furthermore, a new formulation for frictional contact between two spheres is presented. In this new element, similarly to the formulation [7], the contact problem is solved using an augmented Lagrangian formulation [8] which was applied by Galvez *et al.* [9] to dynamic problems with friction. The total motion is directly referred to an inertial frame for the kinematic description of the bodies with large rotations and displacements, as proposed by Géradin and Cardona [10]. Finally, three numerical examples are presented to validate and to evaluate the performance of the method.

2 FRICTIONAL CONTACT PROBLEM

In order to describe the kinematics of two contacting bodies with friction effects, the gap distance between the contact surfaces is usually split into a normal $g_N \in \mathbb{R}$ and a tangential $\mathbf{g}_T \in \mathbb{R}^2$ components with respect to a material orthonormal frame. The same procedure is performed with the contact force $\boldsymbol{\nu}$ which is decomposed into a normal $v_N \in \mathbb{R}$ and a tangential $\boldsymbol{\nu}_T \in \mathbb{R}^2$ components. Thus, the restrictions of gap, contact, stick or slip of the frictional contact problem at position level are given by:

$$\begin{aligned} g_N \geq 0 \quad v_N \geq 0, \quad g_N v_N = 0; \\ \|\mathbf{g}_T\| \geq 0, \quad \|\boldsymbol{\nu}_T\| \leq \mu v_N, \quad \|\mathbf{g}_T\| (\|\boldsymbol{\nu}_T\| - \mu v_N) = 0 \quad \|\boldsymbol{\nu}_T\| \mathbf{g}_T = -\|\mathbf{g}_T\| \boldsymbol{\nu}_T \end{aligned} \quad (1)$$

where μ is the friction coefficient. The first set of inequality equations of Eq.(1) represents the Signorini contact conditions. It indicates if the bodies are in *gap* or in *contact* status. The second set corresponds to the Coulomb friction law that can be either in *stick* or *slip*. The set of inequality constraints in Eq.(1) are satisfied exactly by using the augmented Lagrangian formulation proposed by Alart and Curnier [8]. The adopted form of the augmented Lagrangian function for the frictional contact problem at position level of Eq.(1), in terms of the nodal coordinates vector \mathbf{q} and $\boldsymbol{\nu}$, is given by

$$\mathcal{L}^p(\mathbf{q}, \boldsymbol{\nu}) = -k_p g_N v_N + \frac{p_p}{2} g_N^2 - \frac{\text{dist}^2}{2p_p} [\xi_N, \mathbb{R}^+] - k_p \mathbf{g}_T \cdot \boldsymbol{\nu}_T + \frac{p_p}{2} \|\mathbf{g}_T\|^2 - \frac{\text{dist}^2 [\boldsymbol{\xi}_T, C_{\xi_N}]}{2p_p} \quad (2)$$

where $\xi_N = k_p v_N - p_p g_N$ and $\boldsymbol{\xi}_T = k_p \boldsymbol{\nu}_T - p_p \mathbf{g}_T$ are the augmented multipliers for the normal and the tangential direction at position level, respectively; p_p is a positive penalty parameter and k_p is a scaling factor for the Lagrange multipliers v_N and $\boldsymbol{\nu}_T$. The numerical solution does not depend on the value of these parameters; however, we found that to improve the convergence rate, the default values should be chosen according to $k_p = p_p = \bar{m}$, with \bar{m} a characteristic mass of the problem. The function $\text{dist}(z, C)$ is the distance between a point $z \in \mathbb{R}^n$ and the convex set C while the cone C_{ξ_N} is the convex set defined by the extension of the friction cone $C(k_p v_N + p_p g_N) \equiv C(\xi_N)$ to the half-line $\mathbb{R}^-(\xi_N)$, i.e., the set of negative values of the normal augmented multiplier $\xi_N = k_p v_N + p_p g_N$, more details can be found in [11]. We remark that \mathbf{g}_T is the tangential component of the incremental relative displacement between two points in contact during the considered period of time (the integrator time step).

In a similar way, the frictional contact conditions at velocity level are written as follows:

$$\begin{aligned} \dot{g}_N &\geq 0, \quad \Lambda_N \geq 0, \quad \dot{g}_N \Lambda_N = 0; \\ \|\dot{\mathbf{g}}_T\| &\geq 0, \quad \|\Lambda_T\| \leq \mu \Lambda_N, \quad \|\dot{\mathbf{g}}_T\| (\|\Lambda_T\| - \mu \Lambda_N) = 0 \quad \|\Lambda_T\| \dot{\mathbf{g}}_T = -\|\dot{\mathbf{g}}_T\| \Lambda_T \end{aligned} \quad (3)$$

where $\Lambda_N \in \mathbb{R}$ and $\Lambda_T \in \mathbb{R}^2$ are the normal and the tangential impulses in the normal and tangential directions, respectively, with respect to an orthonormal material frame. The first inequality in Eq. (3) indicates that when impacting, $\dot{g}_N = 0$ and a velocity jump is produced (Newton's impact law in the normal direction); the second one is the non-traction condition (only compression is allowed at impact) and the third one is the complementarity equation. Then, the terms $\dot{g}_N \in \mathbb{R}$ and $\dot{\mathbf{g}}_T \in \mathbb{R}^2$ express the Newton impact's law in the normal and tangential directions. They are given by the following equations,

$$\dot{g}_N = g_{Nq,n+1} v_{n+1} + e_N g_{Nq,n} v_n \quad (= 0) \quad \dot{\mathbf{g}}_T = \mathbf{g}_{Tq,n+1} v_{n+1} + e_T \mathbf{g}_{Tq,n} v_n \quad (= 0) \quad (4)$$

Here, $e_N \in [0, 1]$ and $e_T \in (-1, 1)$ are the coefficients of restitution in the normal and tangential directions, respectively, and g_{Nq} and \mathbf{g}_{Tq} are the gradients of the normal and incremental tangential displacements, respectively. The remark ($= 0$) on the right-hand-side of Eq.(4), indicates that the corresponding equation is zero when convergence is achieved. The second set of restrictions of Eq.(3) gives the impact equations in the tangential direction to consider friction effects. Then, similarly to Eq.(2), the augmented Lagrangian which regularizes the frictional contact problem at velocity level is given by

$$\mathcal{L}^v(\mathbf{v}, \Lambda) = -k_v \dot{g}_N \Lambda_N + \frac{p_v}{2} \dot{g}_N^2 - \frac{\text{dist}^2[\sigma_N, \mathbb{R}^+]}{2p_v} - k_v \dot{\mathbf{g}}_T \cdot \Lambda_T + \frac{p_v}{2} \|\dot{\mathbf{g}}_T\|^2 - \frac{\text{dist}^2[\sigma_T, C_{\sigma_N}]}{2p_v} \quad (5)$$

where $\sigma_N = k_v \Lambda_N - p_v \dot{g}_N$ and $\sigma_T = k_v \Lambda_T - p_v \dot{\mathbf{g}}_T$ are the augmented multipliers at velocity level in the normal and tangential directions, respectively and C_{σ_N} is a section of radius $\mu \sigma_N$ of the augmented Coulomb friction cone expressed in terms of velocity variables. Then, p_v is a positive penalty parameter and k_v is the scaling factor for the Lagrange multipliers Λ_N and Λ_T . Both p_v and k_v are usually chosen with the same values as p_p and k_p , respectively.

The virtual variations of the augmented Lagrangians of Eqs.(2,5) give the internal force vectors, and their linearisation yields the corresponding Hessian matrices, see [9, 7] for a detailed explanation. Here, since the modification required to model multiple collisions with friction are performed only at velocity level, we will focus on the velocity sub-problem. Thus, the virtual variation of Eq.(5) gives the internal force vector at velocity level for the three contact scenarios: gap, stick and slip, and is expressed:

$$\delta \mathcal{L}^v(\Phi) = \delta \Phi^T \mathbf{F}^v(\Phi) \rightarrow \mathbf{F}^v(\Phi) = \begin{cases} \begin{cases} \mathbf{0} \\ -\frac{k_v}{p_v} \Lambda_N \\ -\frac{k_v}{p_v} \Lambda_T \end{cases} & \sigma_N < 0 \quad \text{Gap} \\ \begin{cases} -g_{Nq}^T \sigma_N - \mu \sigma_N g_{Tq}^T \tau_v \\ -k_v \dot{g}_N \\ \frac{k_v}{p_v} (-k_v \Lambda_T + \mu \sigma_N \tau_v) \end{cases} & \|\sigma_T\| \geq \mu \sigma_N \quad \text{Slip} \\ \begin{cases} -g_{Nq}^T \sigma_N - g_{Tq}^T \sigma_T \\ -k_v \dot{g}_N \\ -k_v \dot{\mathbf{g}}_T \end{cases} & \|\sigma_T\| < \mu \sigma_N \quad \text{Stick} \end{cases} \quad (6)$$

where $\Phi = [v \ \Lambda_N \ \Lambda_T]$ is the generalized coordinates vector, \mathbf{v} is the generalized velocities vector and $\tau_v = \sigma_T / \|\sigma_T\|$ is a unit vector that defines the tangential direction of the contact force at velocity level.

3 SPHERE-SPHERE CONTACT MODEL WITH FRICTION

A new sphere-sphere contact element formulation with sliding friction is introduced in this section (Fig.1). The model is developed for three dimensional movements. Each sphere is considered as a point attached to a rigid body element that gives the mass and inertia properties. Then, the kinematics is described by the coordinates (position, orientation) of a body in the space. The element does not increase significantly the number of degrees of freedom of the global system of equations and for this reason, the formulation is computationally efficient and relatively easy to implement into a non linear finite element code. The model is able to capture when the spheres are in contact, rotating or sliding over each other with a relative rotation angular velocity. The kinematic movement is referred to an inertial frame defined by a set of orthogonal base vectors \mathbf{X}_1 , \mathbf{X}_2 and \mathbf{X}_3 . The centre of the sphere A with radius r_A and the centre of the sphere B with radius r_B are located at nodes A and B , respectively. The positions of these nodes at the current time step are given by vectors $\mathbf{x}_{A,n+1}$ and $\mathbf{x}_{B,n+1}$ (Fig. 1).

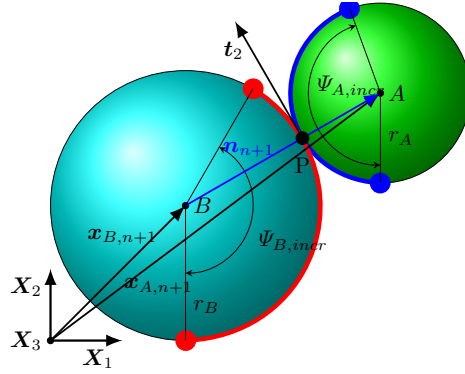


Figure 1. General configuration for the three-dimensional sphere-sphere contact model.

The description of motion of the spheres is completed by giving the incremental rotation vector at nodes A and B from time step n to time step $n+1$, which is represented by the vectors $\Psi_{A,incr} \in \mathbb{R}^3$ and $\Psi_{B,incr} \in \mathbb{R}^3$ as follows

$$\exp(\tilde{\Psi}_{A,incr}) = \mathbf{R}_{A,n}^T \mathbf{R}_{A,n+1} \quad \exp(\tilde{\Psi}_{B,incr}) = \mathbf{R}_{B,n}^T \mathbf{R}_{B,n+1}$$

where the exponential map $\exp(\tilde{\Psi})$ is used. Here, $\Psi_{incr} = \text{vect}(\tilde{\Psi}_{incr})$ is the so-called Cartesian rotation vector which has the direction of the rotation axis and a length equal to the amplitude of the incremental rotation [10] (the operator $\tilde{\mathbf{a}} : \mathbb{R}^3 \rightarrow \mathbb{R}^3 \otimes \mathbb{R}^3$ returns a 3×3 skew-symmetric matrix such that $\mathbf{a} \times \mathbf{b} = \tilde{\mathbf{a}}\mathbf{b} \forall \mathbf{a}, \mathbf{b} \in \mathbb{R}^3$).

In order to calculate the gap vector $\mathbf{g} = [g_N \mathbf{g}_T^T]^T$ of this element, an orthonormal material frame at the contact point P is defined (Fig. 1). It is given by a unit normal vector \mathbf{n} defined from vectors \mathbf{x}_A and \mathbf{x}_B , and two tangential vectors \mathbf{t}_1 and \mathbf{t}_2 perpendicular to \mathbf{n} ,

$$\mathbf{n} = \frac{\mathbf{x}_B - \mathbf{x}_A}{\|\mathbf{x}_B - \mathbf{x}_A\|} \quad \mathbf{t}_1 = \frac{\mathbf{e} \times \mathbf{n}}{\|\mathbf{e} \times \mathbf{n}\|} \quad \mathbf{t}_2 = \mathbf{n} \times \mathbf{t}_1 \quad (7)$$

where \mathbf{e} is an arbitrary vector not collinear with \mathbf{n} . According to Fig. 1, the generalized gap vector is defined as

$$\begin{bmatrix} g_N \\ g_{T1} \\ g_{T2} \end{bmatrix} = \begin{bmatrix} \|\mathbf{x}_{A,n+1} - \mathbf{x}_{B,n+1}\| - (r_A + r_B) \\ \mathbf{t}_{2,n} \cdot (\Psi_{A,incr} r_A + \Psi_{B,incr} r_B) - \mathbf{t}_{1,n} \cdot [(\mathbf{x}_{A,n+1} - \mathbf{x}_{B,n+1}) - (\mathbf{x}_{A,n} - \mathbf{x}_{B,n})] \\ -\mathbf{t}_{1,n} \cdot (\Psi_{A,incr} r_A + \Psi_{B,incr} r_B) - \mathbf{t}_{2,n} \cdot [(\mathbf{x}_{A,n+1} - \mathbf{x}_{B,n+1}) + (\mathbf{x}_{A,n} - \mathbf{x}_{B,n})] \end{bmatrix} \quad (8)$$

where the first component corresponds to the normal gap g_N while the two remaining components represent the incremental tangential movement g_{T1} and g_{T2} . From Eq.(8), $\mathbf{t}_{\alpha,n} \cdot [(\Psi_{A,incr} r_A + \Psi_{B,incr} r_B)]$

with $\alpha = 1, 2$ is related to the relative rotating movement between the spheres. Meanwhile $\mathbf{t}_{\alpha,n} \cdot [(\mathbf{x}_{A,n+1} - \mathbf{x}_{A,n}) + (\mathbf{x}_{B,n+1} - \mathbf{x}_{B,n})]$ is the incremental displacement in the tangential directions. Note that in Eq.(8), the tangential vectors \mathbf{t}_α are evaluated at previous time step in order to facilitate the Hessian matrix linearization. This simplification does not impose a severe restriction to the numerical solutions as we will demonstrate in the numerical examples. To compute the internal force vector at velocity level given in Eq.(6), the Newton impact's law is required. For this element, it takes the following form,

$$\begin{bmatrix} \overset{\circ}{g}_N \\ \overset{\circ}{g}_{T1} \\ \overset{\circ}{g}_{T2} \end{bmatrix} = \begin{bmatrix} \mathbf{n}_{n+1} \cdot (\mathbf{v}_{A,n+1} - \mathbf{v}_{B,n+1}) + e_N \mathbf{n}_n \cdot (\mathbf{v}_{A,n} - \mathbf{v}_{B,n}) \\ \mathbf{t}_{2,n} \cdot (\boldsymbol{\omega}_{A,n+1} r_A + \boldsymbol{\omega}_{B,n+1} r_B) - \mathbf{t}_{1,n} \cdot (\mathbf{v}_{A,n+1} - \mathbf{v}_{B,n+1}) + \\ + e_T [\mathbf{t}_{2,n} \cdot (\boldsymbol{\omega}_{A,n} r_A + \boldsymbol{\omega}_{B,n} r_B) - \mathbf{t}_{1,n} \cdot (\mathbf{v}_{A,n} - \mathbf{v}_{B,n})] \\ -\mathbf{t}_{1,n} \cdot (\boldsymbol{\omega}_{A,n+1} r_A + \boldsymbol{\omega}_{B,n+1} r_B) - \mathbf{t}_{2,n} \cdot (\mathbf{v}_{A,n+1} - \mathbf{v}_{B,n+1}) + \\ + e_T [-\mathbf{t}_{1,n} \cdot (\boldsymbol{\omega}_{A,n} r_A + \boldsymbol{\omega}_{B,n} r_B) - \mathbf{t}_{2,n} \cdot (\mathbf{v}_{A,n} - \mathbf{v}_{B,n})] \end{bmatrix} \quad (9)$$

where \mathbf{v} and $\boldsymbol{\omega}$ are the linear and angular velocities, respectively. By using the gap definition, Eq.(8), and the Newton's impact law, Eq.(9), the expressions to evaluate the internal force vectors and the Hessian matrices in the context of nonsmooth generalized time integrator scheme are obtained. The elementary Hessian matrices and the internal force vectors, both at position and velocity levels, contribute to the global tangent matrices and to the generalized internal forces vectors by a standard assembly procedure.

4 MULTIPLE IMPACTS COLLISION

This section presents the formulation of the algorithm for frictional multiple impacts collisions, which is based on the recent work presented by Cosimo *et al* [12]. Unlike that paper, here the friction effects between the contacting bodies are considered. In Cosimo *et al* [12], the authors proposed a modification to the active set criterion at velocity level in order to use the classical Newton impact's law. By following this methodology, the new multiple impacts active set in the context of the sphere-sphere frictional contact element is given by the expression,

$$\mathcal{G}^* = \overline{\mathcal{U}} \cup \{j \in \mathcal{A} : \overset{\circ}{g}_{Nq}^{*j} \tilde{\mathbf{V}}^- < \text{tol}_v \quad \text{and} \quad \sigma^{*j} \geq 0\} \quad (10)$$

where

$$\tilde{\mathbf{V}}^- = \left[\tilde{\mathbf{V}}_A^{-,T} \quad \tilde{\mathbf{V}}_B^{-,T} \quad \tilde{\boldsymbol{\Omega}}_A^{-,T} \quad \tilde{\boldsymbol{\Omega}}_B^{-,T} \right]^T \quad (11)$$

is the update vector of the pre-impact velocity of $\tilde{\mathbf{v}}$ for the next iterations, thus $\tilde{\mathbf{V}}^- = \mathbf{v}$. Note that the symbol $\tilde{\cdot}$ does not represent the skew symmetric matrix. The choice of the tolerance tol_v is discussed in detail in [12]. Then, the new Newton impact's law in the normal and tangential directions defined for every $j \in \mathcal{C}$ is defined next

$$\overset{\circ}{g}_N^{*j} = g_{Nq,n+1}^j \mathbf{v}_{n+1} + e_N^j g_{Nq,n}^j \mathbf{V}^- \quad \overset{\circ}{g}_T^{*j} = g_{Tq,n+1}^j \mathbf{v}_{n+1} + e_T^j g_{Tq,n}^j \mathbf{V}^- \quad (12)$$

where

$$\mathbf{V}^- = \left[\mathbf{V}_A^{-,T} \quad \mathbf{V}_B^{-,T} \quad \boldsymbol{\Omega}_A^{-,T} \quad \boldsymbol{\Omega}_B^{-,T} \right]^T \quad (13)$$

is the update vector of the pre-impact velocity of \mathbf{v}_n for the next iterations, thus $\mathbf{V}^- = \mathbf{v}_n + \mathbf{W}_{n+1}$. Finally, the modified augmented multiplier at velocity level is defined as,

$$\begin{bmatrix} \sigma_{N,n+1}^* \\ \sigma_{T1,n+1}^* \\ \sigma_{T2,n+1}^* \end{bmatrix} = \begin{bmatrix} k_v \Lambda_N - p_v \overset{\circ}{g}_N^* \\ k_v \Lambda_{T1} - p_v \overset{\circ}{g}_{T1}^* \\ k_v \Lambda_{T2} - p_v \overset{\circ}{g}_{T2}^* \end{bmatrix} \quad (14)$$

The resulting impulses have to be accumulated, taking into account the sequence of impacts at each step. Therefore, the accumulated impulses in the normal and tangential directions are given

by the following equations

$$\mathbf{P}_N = \sum_j^{i-1} \mathbf{g}_{Nq}^{\mathcal{G}_j^*, T} \Lambda_N^{\mathcal{G}_j^*} \quad \mathbf{P}_T = \sum_j^{i-1} \mathbf{g}_{Tq}^{\mathcal{G}_j^*, T} \Lambda_T^{\mathcal{G}_j^*} \quad (15)$$

where the index i is used to denote the impact problem from the sequence of impacts at the current step. Finally, the internal force vector yields

$$\mathbf{F}^{v^*, \mathcal{G}^*}(\Phi) = \begin{cases} \begin{cases} \mathbf{0} \\ -\frac{k_v^2}{p_y} \Lambda_N^{\mathcal{G}^*} \\ -\frac{k_v^2}{p_v} \Lambda_T^{\mathcal{G}^*} \end{cases} & \sigma_N^* < 0 \quad \text{Gap} \\ \begin{cases} -\mathbf{g}_{Nq}^{\mathcal{G}^*, T} \sigma_N^{*\mathcal{G}^*} - \mu \sigma_N^{*\mathcal{G}^*} \mathbf{g}_{Tq}^{\mathcal{G}^*, T} \tau_v - \mathbf{P}_N - \mathbf{P}_T \\ -k_v \mathring{\mathbf{g}}_N^{\mathcal{G}^*} \\ \frac{k_v}{p_v} (-k_v \Lambda_T^{\mathcal{G}^*} + \mu \sigma_N^{*\mathcal{G}^*} \tau_v) \end{cases} & \|\sigma_T^*\| \geq \mu \sigma_N^* \quad \text{Slip} \\ \begin{cases} \mathbf{g}_{Nq}^{\mathcal{G}^*, T} \sigma_N^{\mathcal{G}^*} - \mathbf{g}_{Tq}^{\mathcal{G}^*, T} \sigma_T^{\mathcal{G}^*} - \mathbf{P}_N - \mathbf{P}_T \\ -k_v \mathring{\mathbf{g}}_N^{\mathcal{G}^*} \\ -k_v \mathring{\mathbf{g}}_T^{\mathcal{G}^*} \end{cases} & \|\sigma_T^*\| < \mu \sigma_N^* \quad \text{Stick} \end{cases} \quad (16)$$

5 NUMERICAL EXAMPLES

Three numerical examples are presented to show the accuracy and robustness of the proposed methodology. The contact element algorithms developed in this work has been implemented in the finite element research code Oofelie [13].

5.1 Single Collision Example

This example is proposed to simulate the case of frictional impact between two spheres. The numerical solution is validated against the 30° rule, which is well known in the analysis of billiard balls collisions [14]. The 30° rule states that if a ball in rolling movement (the *cue ball*) impacts between 1/4-ball hit (49° cut) and 3/4-ball hit (14° cut) with an static ball, it will deflect by almost 30° from its original direction after hitting the static ball. The exact cue ball deflection angle θ_c as a function of the cut angle ϕ is given by the following equation,

$$\theta_c = \tan^{-1} \left(\frac{\sin(\phi) \cos(\phi)}{\sin^2(\phi) + \frac{2}{5}} \right) \quad (17)$$

where $\phi = \sin^{-1}(1 - f)$ is calculated from the hit ball fraction factor $f \in [0, 1]$ between the balls. The comparison of this rule with the experimental solutions can be found in [14, 15] and in many videos available in websites. For the simulations, we selected the reference geometrical and physical properties values given by the classical pool/billiard book of Alciatore [14]. The diameter of the balls is 5.71 cm, the mass 0.17 kg, the friction coefficients between the balls and between the balls and the cloth are 0.06 and 0.2, respectively. The normal restitution coefficient value between the balls is 0.93 and it is 1 between the balls and the cloth. The tangential restitution coefficient is 0 for all contact points and the acceleration of gravity is $g = 9.8 \text{ m/s}^2$. Then, an initial velocity of 2 m/s with null angular velocity was imposed to the cue ball. The numerical solution is computed with a spectral radius of $\rho_\infty = 0.8$ and a time step of $1 \times 10^{-3} \text{ s}$. The values of the Newton tolerance for convergence is equal to 1×10^{-5} . Computations with nine different hit ball fraction factors f were proposed to validate the algorithm: [0, 0.125, 0.25, 0.375, 0.5, 0.625, 0.75, 0.875, 1]. Figure 2 shows that the analytic and the numerical solutions are in agreement. For the adopted tolerances, a maximum number of iterations per time-step of 1, 4 and 2 and a mean number of 1 iteration per time-step for each sub-problem were reported.

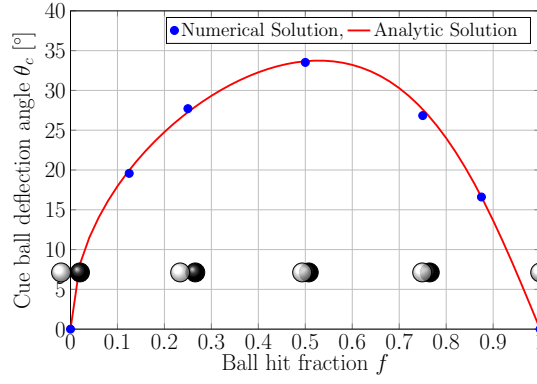


Figure 2. The 30 °rule. Numerical and analytical solution comparison.

5.2 The effect of friction on the throw angle

Throw effects are produced by the friction forces imparted from a moving ball sliding or rotating against a stationary ball. The cue ball (CB) has a spinning angular velocity ω_{CB} and an initial linear shot velocity v^- . Then, the CB impacts with the objective ball (OB) and the latter is deflected with a throw angle θ_{throw} and a post-impact velocity v^+ . Figure 3 shows a schematic drawing of the kinematics of impact between the CB and the OB. From the work of Alciatore [14], the throw

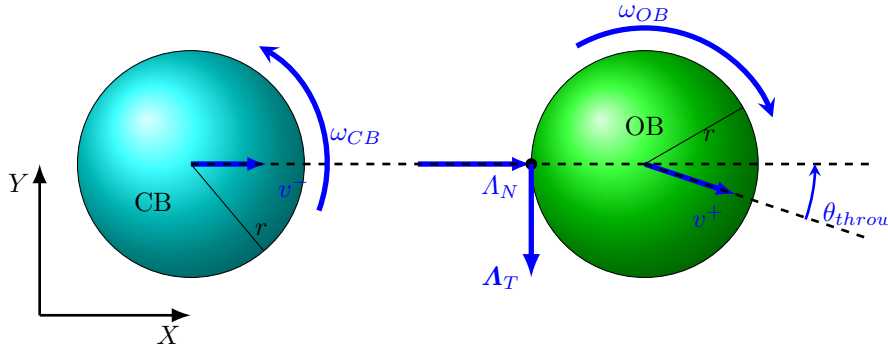


Figure 3. Throw angle effect in two spherical bodies.

angle depends on the speed of the shot v , the cut angle ϕ , the amount and direction of CB spin velocity ω_{CB} , the friction coefficient μ and the radius R of the balls. The analytical equation to calculate θ_{throw} is given by

$$\theta_{throw} = \tan^{-1} \left[\frac{\min \left[\frac{\mu v^- \cos \phi}{v_{rel}}, 1/7 \right] (v^- \sin \phi - R \omega_{zCB})}{v^- \cos \phi} \right] \quad (18)$$

where $v_{rel} = \sqrt{(v^- \sin \phi - R \omega_{zCB})^2 + (R \omega_{xCB} \cos \phi)^2}$ is the initial relative velocity magnitude at the point of impact. Several experiments performed by Jewett [16] and Alciatore [17, 18] have verified the validity of Eq.(18). For the numerical experiment, typical values for billiard balls are taken from [14]. Both the CB and the OB have a radius of $R = 0.028575$ m, a mass of $m = 0.17$ kg and are subjected to a gravity acceleration of $g = 9.8$ m/s². The friction between the balls and the plane is neglected in order to consider in the simulations only the spin movement which is transferred from the CB to the OB. Then, different angular velocities for the CB were proposed: $\omega_{zCB} = [-58.59, -46.89, -35.17, -23.44, -11.72]$ rad/s together with the following friction coefficients between the spheres $\mu = [0.039, 0.048, 0.059, 0.074, 0.093]$ corresponding to each ω_{zCB} . The velocity of the CB was $v^- = 1.341$ m/s in the x direction. The time step used in the simulations was 1×10^{-4} s, and the total time for the simulation was 0.5 s. The value of tolerance

for checking the Newton solver convergence was equal to 1×10^{-5} and the spectral ratio selected is $\rho_\infty = 0.8$. Figure 4 shows a comparison between the throw angle θ_{throw} as a function of $R\omega_z/v^-$

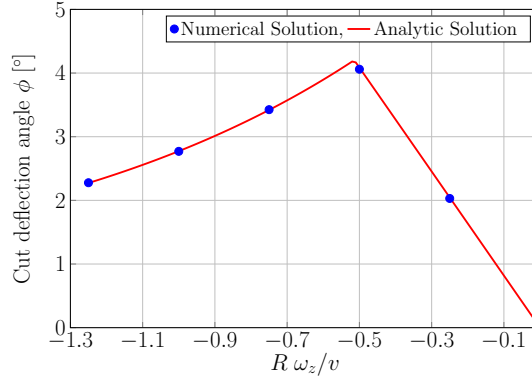


Figure 4. Throw angle for different friction coefficients.

calculated with Eq.(18) and the numerical solution computed in this work. As Fig.4 shows, both solutions are in a good agreement. For this example, the maximum number of iterations per time-step was 1, 3 and 3 for the smooth, position and velocity sub-problems, respectively. The mean number of iterations was 1 per time-step for each sub-problem.

5.3 Pool balls interaction

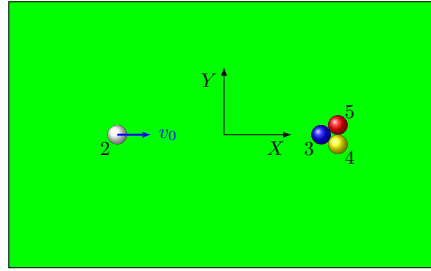
This numerical example was initially proposed by Gismeros *et al.* [19]. It consists in a typical billiard break which allows to study the capacity of the algorithm to solve problems with multiple impacts with and without friction. According to [19], a white ball labeled 2 with a speed of $v_x = 10.792$ m/s hits three balls labeled 3, 4 and 5 that are in contact between them and at rest (see Fig. 5-a). The four balls have a radius $R = 0.028575$ m, a weight $mg = 1.666$ N and an inertia $I = 0.000055$ kg m². The table has a length of 2.54 m and a width of 1.27 m [20]. The values of the friction coefficient μ and the normal restitution coefficient e_N are 0.2 and 0, respectively, for the contact between the spheres and the table. The coefficients for the contact between spheres are $\mu = 0.06$ and $e_N = 0.93$ while for the contact between the spheres and the edges of the table, $\mu = 0$ and $e_N = 0.85$. In all contact points a tangential restitution coefficient $e_T = 0$ is imposed.

Two cases are analyzed: in the first one, the rolling resistance between the spheres and the plane is neglected, while in the second one a rolling resistance radius $\rho = 0.005$ m is adopted. The total simulation time was 3 s with a time step of 1×10^{-3} s. In the first case, the cue ball starts with a velocity of 10.729 m/s and null rolling velocity, and impacts the balls at a slightly lower velocity due to the sliding friction between the ball and the plane, see Fig. 5-b. After multiple impacts, ball 3 moves forward with a low velocity. As it can be seen, once the balls are in pure rolling, their velocity remains constant (Fig. 5-b). The second case is similar to the first; however, the balls reach the rest condition due to the action of the rolling resistance, see Fig. 5-c.

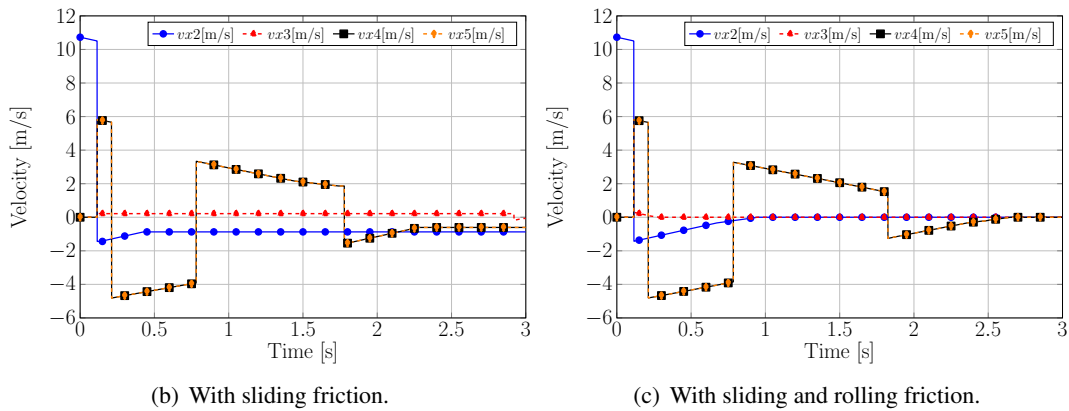
The results show that the proposed methodology does not present any penetration between bodies in contact, contrary to what happened using the methodology given by Gismeros *et al.* [19] based on the penalty approach. Furthermore, the computing time was reduced from 25000 s, as demanded in the case of Gismeros *et al* to only 40 s.

6 CONCLUSIONS

A new methodology for handling simultaneous multiple impacts with friction effects between spherical rigid bodies was presented. The algorithm is based on the frictionless proposal by Cosimo *et al.* [5] in which the Newton impact law is sequentially applied by assuming instantaneous local impact times. Then, a detailed kinematic formulation of a spherical-spherical frictional



(a) Billiard break configuration.



(b) With sliding friction.

(c) With sliding and rolling friction.

Figure 5. Numerical example: billiard break

contact element by using large rotations and absolute coordinates is presented. The studied examples demonstrated that the proposed methodology keeps a low computational cost compared with the classical penalty approaches. Furthermore, the strategy does not require any intervention of the user or any topological analysis for defining the sequence for processing the multiple impacts.

ACKNOWLEDGEMENTS

This work received financial support from Consejo Nacional de Investigaciones Científicas y Técnicas (CONICET) PIP11220200101688CO and Universidad Tecnológica Nacional PID-UTN AMECAFE0008102TC which are gratefully acknowledged.

REFERENCES

- [1] Liu, C., Zhao, Z., Brogliato, B.: Frictionless multiple impacts in multibody systems. II. Numerical algorithm and simulation results. *Proceedings of the Royal Society A: Mathematical, Physical and Engineering Sciences* **465**(2101) (2009) 1–23
- [2] Nguyen, N.S., Brogliato, B.: *Multiple impacts in dissipative granular chains*. Volume 72. Springer Science & Business Media (2013)
- [3] Darboux, G.: Étude géométrique sur les percussions et le choc des corps. *Bulletin des Sciences Mathématiques et Astronomiques* **4**(1) (1880) 126–160
- [4] Liu, C., Zhao, Z., Brogliato, B.: Frictionless multiple impacts in multibody systems. I. Theoretical framework. *Proceedings of the Royal Society A: Mathematical, Physical and Engineering Sciences* **464**(2100) (2008) 3193–3211
- [5] Cosimo, A., Cavalieri, F.J., Cardona, A., Brüls, O.: On the adaptation of local impact laws for multiple impact problems. *Nonlinear Dynamics* **102**(4) (2020) 1997–2016

- [6] Cosimo, A., Galvez, J., Cavalieri, F.J., Cardona, A., Brüls, O.: A robust nonsmooth generalized- α scheme for flexible systems with impacts. *Multibody System Dynamics* **48**(2) (2020) 127–149
- [7] Cavalieri, F.J., Cosimo, A., Sanchez, E., Brüls, O., Cardona, A.: Simulation of sliding friction of spherical rigid bodies subject to multiple impact collisions. In Pucheta, M., Cardona, A., Preidikman, S., Hecker, R., eds.: *Multibody Mechatronic Systems*, Cham, Springer International Publishing (2021) 151–158
- [8] Alart, P., Curnier, A.: A mixed formulation for frictional contact problems prone to Newton like solution methods. *Comput. Methods Appl. Mech. Eng.* **92**(3) (1991) 353–375
- [9] Galvez, J., Cavalieri, F.J., Cosimo, A., Brüls, O., Cardona, A.: A nonsmooth frictional contact formulation for multibody system dynamics. *Int. J. Numer. Methods Eng.* **121**(16) (2020) 3584–3609
- [10] G eradin, M., Cardona, A.: *Flexible Multibody Dynamics: A Finite Element Approach*. Wiley (2001)
- [11] Leine, R.I., van de Wouw, N., eds.: *Stability and Convergence of Mechanical Systems with Unilateral Constraints*. Springer Berlin Heidelberg (2008)
- [12] Cosimo, A., Cavalieri, F.J., Cardona, A., Brüls, O.: On the adaptation of local impact laws for multiple impact problems. *Nonlinear Dynamics* **102**(4) (2020) 1997–2016
- [13] Cardona, A., Klapka, I., G eradin, M.: Design of a new finite element programming environment. *Engineering Computations* **11** (1994) 365–381
- [14] Alciatore, D.: *The Illustrated Principles of Pool and Billiards*. First edn. Sterling (2017)
- [15] Wallace, R., Schroeder, M.: Analysis of billiard ball collisions in two dimensions. *American Journal of Physics* **56**(9) (1988)
- [16] Jewett, B.: Seeking truth of beliefs. Technical report, Tech Talk, Billiards Digest (1995)
- [17] Alciatore, D.: Throw - Part II: follow and draw effects, Dr. Dave’s illustrated principles. *Billiards Digest* **29**(10) (2006)
- [18] Alciatore, D.: Throw - Part III: follow and draw effects, Dr. Dave’s illustrated principles. *Billiards Digest* **29**(11) (2006)
- [19] Gismeros Moreno, R., Corral Abad, E., Meneses Alonso, J., G omez Garc ıa, M.J., Castej on Sisam on, C.: Modelling multiple-simultaneous impact problems with a nonlinear smooth approach: pool/billiard application. *Nonlinear Dynamics* **107**(3) (2022) 1859–1886
- [20] Alciatore, D.G.: *The illustrated principles of pool and billiards*. Dr. Dave Billiards Resources (2004)